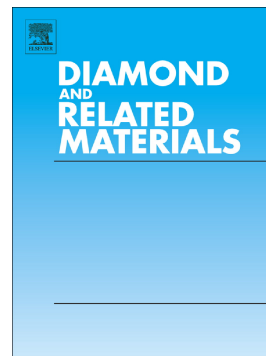# Journal Pre-proof

HP-CNT/TiO2 binary nanohybrids as highly efficient, selective and sustainable photocatalysts for organic transformations under visible light irradiation

Honey Mary Joseph, Hariprasad Narayanan, S. Sugunan

Please cite this article as: H.M. Joseph, H. Narayanan and S. Sugunan, HP-CNT/TiO2 binary nanohybrids as highly efficient, selective and sustainable photocatalysts for organic transformations under visible light irradiation, *Diamond & Related Materials* (2024), https://doi.org/10.1016/j.diamond.2024.111904

This is a PDF file of an article that has undergone enhancements after acceptance, such as the addition of a cover page and metadata, and formatting for readability, but it is not yet the definitive version of record. This version will undergo additional copyediting, typesetting and review before it is published in its final form, but we are providing this version to give early visibility of the article. Please note that, during the production process, errors may be discovered which could affect the content, and all legal disclaimers that apply to the journal pertain.

© 2024 Published by Elsevier B.V.

HP-CNT/TiO₂ binary Nanohybrids as Highly Efficient, Selective and Sustainable Photocatalysts for Organic Transformations under Visible Light Irradiation

Honey Mary Joseph[a,b], Hariprasad Narayanan[c,d], S. Sugunan[a]*

a. Department of Applied Chemistry, Cochin University of Science and Technology, Cochin-682022, Kerala, India.

b. Department of Chemistry, Government College Kottayam- 686013, Kerala, India

c. National Centre for Catalysis Research, Department of Chemistry, IIT Madras, Chennai 600036, Tamil Nadu, India

d. School of Environmental Studies, Cochin University of Science and Technology, Cochin-682022, Kerala, India

*Corresponding author

Dr. Honey Mary Joseph

Lecturer

Department of Applied Chemistry

Government College Kottayam

Kottayam, Kerala-686013

Tel: +91 9074030104

honeymaryjoseph6@gmail.com

Abstract

The manuscript demonstrates the scope of utilizing the green and sustainable strategy of visible light photocatalysis for selective organic transformations at room temperature and mild reaction conditions. Herein, we report the facile synthesis and application of binary hybrid nanocomposites of TiO_2 and functionalized MWCNTs for the reduction of nitrobenzene to aniline and one-pot redox synthesis of 2-substituted benzimidazoles from o-nitroaniline, using different alcohols. The environmentally benign photocatalyst system was prepared by a simple two-step reaction involving the functionalization of MWCNTs with the mild and green oxidant H_2O_2, followed by hydrothermal synthesis. The low cost, hydrogen peroxide functionalized multiwalled carbon nanotubes served as efficient cocatalysts in the reactions. The characterization of the hybrid using XPS, Raman and PL spectra showed the heterojunction structure, Ti-C and Ti-O-C bond formation and oxygen vacancies, trivial for enhancing the charge separation, making the electrons more available for the redox reactions. The TCNT(0.5) nanohybrid with MWCNT content 0.5 wt. %, exhibits the best photocatalytic activity among the reactions investigated, showing about complete(100 %) conversion of substrates in limited time with excellent selectivity.

Keywords: *Hydrogen peroxide functionalized MWCNT (HP-CNT), TiO$_2$, Visible light, Photocatalytic reduction, Nitrobenzene (NB), redox synthesis, Benzimidazole*

1. Introduction

The synthesis of organic compounds like aromatic amines, benzimidazoles and their derivatives are of great significance. They are important intermediates in the manufacture of pharmaceuticals, agrochemicals, dyes, veterinary medicines, cosmetics etc.[1-4]. The industrial production of these chemicals involves the use of harmful reagents and precious

transition metals, despite their high price and scarcity [5]. In the eternal pursuit for green solutions towards environmental pollution and energy crisis, semiconductor photocatalysis has emerged to be a promising strategy. Owing to its numerous advantages including (i) mild reaction conditions of room temperature and atmospheric pressure, (ii) toxic metal free catalysis, (iii) utilization of the natural resources like atmospheric oxygen as oxidant and solar light (UV & visible) as the energy source and (iv) use of alcohols as substrates/solvents (cheap and stable) instead of harmful organic solvents [6], designing, robust, cost effective, environmentally benign and earth abundant photocatalysts with maximum solar energy conversion is of keen interest among the researchers. Various semiconductor materials like TiO_2, ZnS, Fe_2O_3, CeO_2, ZnO, and g-C_3N_4 etc. are investigated as green alternatives for selective organic transformations [7, 8]. However, promising results were obtained, only by doping them with noble metals and transition metals like Au, Pt, Co, Pd, Ru etc. Also, the selectivity of the aforementioned catalyst systems was not remarkable [7, 8]. The enhancement of photocatalytic properties employing various carbon nanostructures has evoked great interest among the scientists in the past decades. There are considerable reports in the literature, where carbon nanostructures are demonstrated as metal free catalysts for various reactions [9, 10]. Their excellent characteristics like electron storage capacity, large surface area, high electronic and thermal conductivity, low fabrication cost, chemical/thermal stability etc. contributed to their extensive application in various streams of science and technology [9, 10]. After the graphene boom, the scientific community neglected its forbearers, CNTs. Zhang *et al.* in their various works projected this problem, but it was seldom addressed. Wu *et al.* has reported the reduction of nitroarenes employing carbon nanotubes functionalized with hydrogen peroxide. They demonstrated that the nature of surface functionalities highly influenced catalytic performance [11]. Another article published by their group in 2014, had demonstrated the significance of electron transfer and absorptive properties of the conjugated

π systems, in the reduction process. However, the reactions were performed at temperature 70 °C and 100 °C in presence of toxic hydrazine monohydrate [12, 13]. In 2015, Hu *et al.* studied the structural and mechanistic aspects of hydrogenation of nitrophenol employing amino acid modified graphene carbocatalysts [14]. Even though, researches on photocatalysis, employing CNTs in pollutant degradation and hydrogen generation were performed extensively, their application in selective organic transformations is still lacking [15-18].

MWCNTs are projected as effective cocatalysts in photocatalytic organic transformations and can render effective and economic synthetic route for fine chemical synthesis, via net reductive, net oxidative and redox neutral reactions [11, 12]. The high specific absorption capability of carbon nanostructures like CNT, graphene etc. can be attributed to their large surface area, electronic polarizability and surface hydrophobicity of these nanostructures that assist the adsorption of the strong electron accepting and highly polar nitroarenes [19]. MWCNTs has evoked our interest due to their low cost, wide availability, easy processability, high chemical stability, good adsorption properties, high electron storage capacity, excellent electronic and thermal conductivity, high specific surface area, and functionalizable surfaces. The properly functionalized CNTs perform the multifunctional role of reducing the band gap, enhancing charge separation, serving as absorptive sites (surface defects, edge sites and conjugated π systems) and diffusion sites (surface hydroxyl, carbonyl groups) [11, 12, 20].

Inspired by the aforementioned studies in literature, we have investigated the visible light insensitivity and the low nitroarene absorption of TiO_2 and have observed great enhancement in the photocatalytic efficiency of TiO_2, by inducing proper synergy between the two components TiO_2 and Multiwalled carbon nanotubes (mwcnts). Herein, MWCNTs functionalized with hydrogen peroxide (HP-CNTs) are demonstrated as the key and the efficient cocatalyst for two important photocatalytic organic transformations under visible light

irradiation. The reactions under investigation include reduction of nitrobenzene to aniline and redox synthesis of benzimidazoles from ortho-nitro aniline and green solvents like alcohols. Both the reactions were carried out at room temperature under inert atmosphere, employing green solvents like alcohol (hydrogen donor). The activity of the prepared binary hybrid systems was compared with the standard Aldrich titania and the bare lab synthesized titania under visible light. The effect of various parameters like reaction conditions, solvent effect, catalyst amount, time and reusability were investigated in the current study. Furthermore, the structural and mechanistic aspects were studied by proper understanding and correlation of surface characterization and activity studies. To the best of our knowledge, this is the first report of visible light driven photocatalytic synthesis of aniline and redox synthesis of benzimidazoles employing a simple and environmentally benign photocatalyst [carbon nanostructure (MWCNT)/TiO$_2$ binary nanohybrid system] with high selectivity and conversion.

2. Experimental

Details of materials, methods and reagents used are provided in the supporting information. Methods of synthesis of other catalytic systems (not mentioned in section 2.1) probed in the reactions are also provided in the supplementary information.

2.1 Preparation of MWCNT/TiO$_2$ Binary Nanohybrids

The MWCNT/TiO$_2$ binary hybrids with mid-bandgap states were prepared by a green and robust strategy of hydrothermal method. Prior to the synthesis, the MWCNTs were functionalized with the mild and green oxidant H$_2$O$_2$ for the attachment of surface functionalities particularly hydroxyl and ketonic groups. For functionalizing, 1 gram of MWCNTs were well dispersed in 100 ml of 30% H$_2$O$_2$ solution via sonication. Further, it was refluxed at a temperature of 60°C for 5 h. It was then filtered, washed with deionized (DI) water and dried at 80°C overnight to obtain the hydrogen peroxide functionalized MWCNTs (HP-CNTs).

The HP-CNTs were dispersed in 100 ml of IPA by sonicating for 2 hours. Subsequently, 10 ml Titanium Isopropoxide (TIP) dissolved separately in IPA, was further added slowly to this homogenous dispersion with stirring and 5 ml of water was then added into the mixture. The mixture was homogenized by stirring for 24 h. The sol was then transferred into a Teflon lined 500 ml, stainless steel autoclave and was hydrothermally treated at 180 ◦C for 24 h. The obtained slurry was filtered and thoroughly washed with distilled water and finally dried at 60 ˚C overnight to obtain HP-CNT/TiO$_2$ binary nanohybrids.

First, we have randomly chosen 1 wt. %, 5 wt. % and 10 wt. % of MWCNT based catalyst systems. We observed that the 1 wt. % catalyst gave the maximum reactant conversion. We understood that increasing the wt. % of MWCNT would not have a positive impact on the photocatalytic pathway. Hence, for further optimization, we chose the photocatalysts with wt. content of MWCNTs less than 1 wt. %.

The binary hybrids were prepared in varying compositions and they are depicted as TCNT(x), where x denotes the weight percent of MWCNTs incorporated in the photocatalyst. The list of prepared binary MWCNT/TiO$_2$ photocatalysts (TCNT(x)) are listed below.

Table 1 Prepared binary MWCNT/TiO$_2$ photocatalysts (TCNT(x)

2.2 Photocatalytic reaction procedure

Both the reactions, photocatalytic reduction of NB and the redox synthesis of benzimidazoles were performed in a sealed batch type deaerated, cylindrical, round bottomed reactor of 100 ml capacity under visible light irradiation. Uniformly illuminated Oriel Arc lamp system with 150 W Xenon ozone free arc lamp was used as the light source. A 420–630 nm dichroic mirror (cold mirror) filter was used in order to get visible radiation, which gave an irradiance of 96.8 mW/cm^2. Prior to the irradiation, the reaction mixture was purged with N$_2$ for 45 minutes to remove the dissolved oxygen. After the irradiation, the solution was filtered

by a nylon millipore filter (pore size: 0.22 μm) to remove the catalyst particulates. The solution was then analysed by Agilent 7890 GC system. The mass data of the products were determined by GC-MS analyser equipped with 5975C inert MSD with Triple-Axis Detector. The image of the designed photoreactor is provided in the supplementary information (Fig. S1).

3. RESULTS AND DISCUSSIONS

3.1 PHYSICO CHEMICAL CHARACTERIZATION

Figure 1 displays the Raman spectra of MWCNT and MWCNT/TiO$_2$ binary nanohybrids. The nanohybrid photocatalysts exhibited characteristic peaks of both anatase TiO$_2$ as well as G band and D band of MWCNTs. The dominant crystalline phase observed in the binary hybrid system is anatase, which was consistent with the XRD results. It showed the characteristic peaks at 144 cm^{-1}, 197 cm^{-1}, 399 cm^{-1}, 516 cm^{-1} and 630 cm^{-1} corresponding to E_{1g}, E_{2g} B_{1g}, A_{1g} and E_{3g} energy states respectively. Unlike the XRD, Raman spectra is more sensitive to MWCNTs, it shows signature peaks corresponding to MWCNTs even at a low loading of 0.5 wt. %. The intensity of these peaks was found to be increasing in intensity with the increase in weight % of MWCNTs. This clearly confirmed the presence of MWCNTs in the hybrid system. The position of the D band and G band of the pristine MWCNTs had shifted from 1339.6 cm^{-1} and 1563.7 cm^{-1} to 1343.3 cm^{-1} and 1573 cm^{-1} respectively in the hybrid. The evident coexistence of both species (TiO$_2$ and MWCNT) and the shift in the band positions indicate the interfacial synergy that bring about the enhancement in charge transfer between the two species and can contribute to the separation of electron-hole pair [21, 24, 25].

Fig. 1 Raman spectra of prepared TCNT(x) binary nanohybrids

The XRD pattern of the catalyst systems depicted anatase as the major phase of titania present and also, peak corresponding to MWCNTs was not visible due to its low content. It was observed that the crystallite size decreased with increase in

MWCNT content (Table S1). The discussion in detail is provided in the supplementary material (Fig S2).

The photoresponse of the synthesized binary nanohybrid systems were recorded and the UV- Visible absorption spectra are depicted in Fig. 2. The hybrid systems exhibited red shift in the absorption edge upon the increse in MWCNT incorporation (Fig. 2 and Table 2). It was evident that the TCNT(0.3), TCNT(0.5) binary nanohybrids maintained the photoresponse similar to the bare anatase titania (Fig. 2(A:b,c)). The absorbtion edge wavelenghts were determined by extrapolating the parent absorption graphs of each system. It was then utilized to determine the band gap of photocatalysts employing the modified form of Kubelka-Munk equation.

$$Eg = h\nu = \frac{hc}{\lambda} = 1240/\lambda$$

Here, Eg represents the band gap (eV), h is the Planck's constant and λ is the absorption edge wavelength (nm). The TCNT(0.7) exhibited diffuse reflectance with Urbach's tail depicting the formation of mid-bandgap states (Ti-O-C) [26]. The optical band gap calculations for systems above 0.7 wt. % is a matter of dispute as they showed spectra of biphasic systems indicating the segregation of CNTs in the TiO_2 matrix. However, the apparent band gap was calculated by extrapolating the TiO_2 absorption edge (Urbach's tail) in these systems. It was observed that the increase in the MWCNT content, led to the considerable reduction in band gap from 0.1 wt. % to 10 wt. %. The UV-Vis DRS spectra unveils the surface integration of HP-CNTs and TiO_2, consequently depicting the reducion in band gap energy and enhancement in charge carrier mobility [27].

The UV-Visible DRS spectra indicates that the HP-CNTs form intermediate doping states (Ti-O-C) within the TiO_2 band gap. This would in turn permit the excitation of electrons from the inermediate states upon visible light irradiation. Also, it can be noted that the MWCNTs

depict broad absorption in the UV-visible wavelenghth range (Fig.2 (B)). Thus, they can behave as photosensitizers by absorbing the visible light and can inject electrons into the conduction band of TiO_2, thereby transforming the system into visible light active photocatalyst [28, 29]. However when the MWCNT content was increased to 0.7 wt. % (even though the content is comparitively lower) in the binary nanohybrid system, the photoresponse ot the hybrid shifted from the titania type (UV region only) to that of the MWCNT type (broad absorption in UV-visible region). In Fig. 2(A:(d)) the transition state of optical response from the titania type to the MWCNT type is clearly observed. This observation can be attributted either to the formation of mid-bandgap states (Ti-O-C) in the system (TCNT(0.7) or probably due to the beginning of segragation of MWCNTs, making the binary hybrid sytem to be biphasic. The TCNT(1), TCNT(5) and TCNT(10) binary nanohybrids exhibited broad absorption in the UV-visble region, depicting the coexistance of titania and CNT phases distinctly. In light of the above observations, it was inferred that the HP-CNTs (In TCNT(x=0.1- 0.7 wt. %) serve as species that induce the mid-bandgap states (Ti-O-C) and aid the spectral shift, by the absorption of energy lower than the optical band gap, via the phenomenon of enhanced sub-bandgap absorption [26]. The tail (Urbach's tail) in the DRS spectra that depicts the absorption of photons with lower energy than the optical bandgap also indicates the presence of disorders or defects that would form localized states in the sub-bandgap region.The further studies by XPS and PL spectra also provide evidence for the presence of the mid-bandgap states.

While in hybrids with HP-CNT content above 0.7 wt. %, where the surface segregation of MWCNTs was observed, probably the HP-CNTs would act as sensitizers and inject electrons to the CB of titania. Also, the surface integration between HP-CNTs and TiO_2 or the heterojunction formation would not be as efficient as in TCNT(x=0.1 to 0.7 wt. %) binary

hybrids. This was an interesting and unique observation and it provides new insights into the photocatalytic reduction studies of MWCNT based titania systems.

Fig. 2 UV-Vis DRS spectra of prepared TCNT(x) binary nanohybrids

Table 2 Absorption edge and band gap energies of TCNT(x) binary hybrids

The Photoluminescence spectra in the MWCNT/TiO$_2$ nanohybrid originates from the recombination of electrons and holes at the trap sites located at the oxygen vacancies/surface defects or non-coordinated Ti sites [30]. The increase in MWCNT content decreased in PL intensity indicating the reduction in electron-hole recombination [31]. The decrease in PL intensity depicted the direct contact and interaction between MWCNTs and titania, probably through Ti-O-C bonds (XPS spectra) [30]. The PL spectra exhibited a major peak around 400 nm and minor peaks around 450-470 nm, corresponding to the near band gap (NBE) and deep level emissions (DLE) respectively (Fig. 3). The NBE and DLE symbolizes the band gap energies and intrinsic structural defects/vacancies in the binary nanohybrid system respectively [32, 33]. It was noted that two types of defect sites (at 450 nm and 470 nm) were observed in the TCNT(0.1), TCNT(0.3) and TCNT(0.5) nanohybrids. The defect site emission at 450 nm was more pronounced in the TCNT(0.5) nanohybrid clearly elucidating the presence of oxygen vacancies. There are literature reports suggesting the formation of oxygen vacancies upon carbon doping [34]. The florescent emissions corresponding to structural defects/vacancies were not so prominent in the binary nanohybrids with high MWCNT content (above 0.7 wt. %).

Fig. 3 Photoluminescence spectra of prepared TCNT(x) binary nanohybrids

The surface area of the bare lab synthesized titania and the binary nanohybrids were measured using Brunauer-Emmett-Teller (BET) method. The other characteristics like pore volume, pore diameter etc. were also determined and is presented in Table 3. It was evident that the modification of titania with MWCNTs enhanced the textural characteristics like

specific surface area, pore volume and pore diameter of titania significantly. The TCNT(0.3) and TCNT(0.5) binary hybrids exhibited very large specific surface area (around 190 m^2/g) compared to the other binary hybrids. This can be accounted to the superior and effective dispersion of titania nanoparticles on surface functionalized MWCNTs (with H_2O_2). They also possessed greater pore volume and pore diameter. Thus, these hybrids promise more surface active sites and better diffusion of substrates for efficient photocatalytic activity. An increase in surface area was observed when the weight content of MWCNTs was increased from 0.7 wt. % to 10 wt. %. However, there was no pronounced increment in pore volume and pore diameter.

The pore size distribution was also determined from the N_2-adsorption desorption isotherm employing the BET surface area analyser. Fig. 4(a) and (b) depicts the adsorption isotherm and pore size distribution of the TCNT(0.5) photocatalyst. It shows Type IV isotherm (P/P$_0$ range: 0.5 to 0.8) with H2 type (ink bottle type) mesopores (Fig. 4(a)). It's corresponding pore size distribution depicted that the pores were ranging from 2 nm to 4 nm, with the maximum number of pores possessing a diameter of 2.8 nm (Fig. 4(b)).

Fig. 4 (a) N_2 adsorption–desorption isotherm, (b) pore size distribution curve of TCNT (0.5) nanohybrid

Table 3 Textural characteristics of the prepared TCNT(x) binary nanohybrids

The FT-IR spectra of the prepared binary MWCNT/TiO$_2$ nanohybrids are presented in Fig. S3.

The Scanning Electron Micrographs of the pristine MWCNTs, lab synthesized titania and the prepared binary nanohybrids are provided in supplementary material (Fig. S4).

The HR-TEM images of TCNT(0.5) and TCNT(10) hybrids are depicted in Figure 5(a), (b), (c) and (d) respectively. The TiO$_2$ particles in the TCNT(0.5) exhibited uniform cuboidal morphology, while the TCNT(10) exhibited different morphologies. The TEM image of

TCNT(10) depicted particles of spherical, cuboidal and even irregular shaped morphologies. This can be co-related to the biphasic nature of the TCNT(10) binary nanohybrid while the evident attachment of uniform TiO_2 nanoparticles onto the HP-CNTs points to the probability of effective formation of heterojunctions in the TCNT(0.5). This is again well-correlated with the UV-Visible DRS spectra.

Fig. 5 HRTEM images of TCNT(0.5): (a), (b) and TCNT(10): (c), (d) binary nanohybrids

The chemical state and the surface interaction between MWCNTs and titania was further probed, employing X-ray Photoelectron Spectroscopy (Fig. 6). The survey scan of the TCNT(0.5) binary nanohybrid showed peaks corresponding to the elements: carbon, oxygen and titania (Fig. 6(a)).The core level C1s spectrum was deconvoluted to generate five constituent peaks (Fig. 6(b)). The major peak at 284.7 eV arise from the sp^2 carbon (C=C) and the minor peak at 285.5 can be ascribed to the C-C bonds in the carbon skeleton of MWCNTs. The peak around 286.3 eV corresponds to the C-O bonds on the MWCNT surface that serve as anchoring sites for TiO_2 nanoparticles in the binary hybrid system [35]. The peaks at 283.8 eV and 288.6 eV are attributed to the Ti-C and Ti-O-C bonds depicting the chemical bonding between HP-CNTs and TiO_2[36, 37]. This confirms that these bonds can serve as channels for efficient charge transfer and also form intermediate energy states within the TiO_2 band gap to sensitize visible light absorption in the binary hybrid photocatalyst [38]. Herein, correlating with the diffuse reflectance spectra (Fig. 2), it is indicated that the Ti-O-C and Ti-C bonds are formed by replacing the Ti and O atoms in the titania lattice (Ti-O-Ti). Thus the carbon atoms of the MWCNTs are doped into the titania crystalline lattice in the hydrothermally prepared HP-CNT/TiO_2 binary nanohybrid system [39, 40, 41]. The surface treatment and functionalization of the MWCNTs with hydrogen peroxide is the major factor that brought about efficient spatial transport of electrons and holes through the formed HP-CNT-TiO_2 heterojunction. The deconvoluted Ti2p core level spectra exhibit peaks at 458.2 eV, 458.6 eV corresponding to the

$2p_{3/2}$ levels of Ti^{3+} and Ti^{4+} oxidation states. The peaks depicting the $2p_{1/2}$ levels of Ti^{3+} and Ti^{4+} species were observed at 463.3 and 464. 3 eV respectively (Fig. 6(c)). The surface hydroxyl (OH), carbonyl and acidic (O-C=O) groups on the surface of MWCNTs would possibly form bonds with Ti^{4+} atoms reducing the oxidation state of titania to Ti^{3+} during the solvothermal (IPA + water) synthesis [42]. The formation of Ti-C, Ti-O-C bonds lead to the creation of localized states below the TiO_2 conduction band, thereby enhancing the absorption in the visible region and also accounts for the decreased charge transfer resistance and also better charge separation [43, 44]. A minor peak observed at 460.2 eV and 465.3 eV signifies the $2p_{3/2}$ and $2p_{1//2}$ levels of Ti-C bonds. This is a corresponding signature peak of Ti-C bond observed at 283.8 eV in the C1s spectra. Finally, the deconvoluted O1s core level spectra (Fig.6 (d)) show two distinct peaks. The peaks at 529.8 eV and 531.5 eV depicts Ti-O and C-O species present in the binary nanohybrid respectively [36,45]. Thus, the XPS spectra provided insights to the probable modes of interactions in the binary nanohybrid photocatalysts. Our studies provided new insights that both the C doping effect as well as the synergistic interaction through the surface functionalities at the heterojunction is co-existing in the hybrid. This could probably account for the enhanced photocatalytic activity of the hybrid under visible light irradiation.

Fig. 6 XPS spectra of TCNT(0.5) nanohybrid

3.2 PHOTOCATALYTIC INVESTIGATION

3.2.1 Reduction of NB to aniline

The aim of the present study was to synthesize robust and green catalyst systems, for the photocatalytic reduction of NB to aniline. The activity studies under visible light irradiation revealed that the conversion of NB to aniline was exclusively photocatalytic, since no products were obtained when the reaction was done in the absence of light. Also, studies show that the

reaction did not occur without a catalyst. Optimization shows that the reaction was not feasible under air and O_2 atmosphere (Table 4, entry 4, 5). However, 94 % conversion was achieved under N_2 atmosphere (0.02 W/cm^2) employing the TCNT(1) catalyst. The inert atmosphere is maintained to prevent the loss of electrons by the formation of superoxide $[O_2^{2-}]$ anions, or else it would compete with NB for reduction [46,47].

Table 4 Effect of reaction conditions on reduction of NB to aniline

The various photocatalyst systems studied include bare lab synthesized TiO_2, Aldrich titania (anatase: $SATiO_2$), Nf-CNT/TiO_2 binary hybrid (Nf-CNT: nitric acid functionalized MWCNT), HP-CNT/TiO_2 ((TCNT(x)) binary nanohybrid systems, transition metal modified (TM) titania and ternary TM/MWCNT/TiO_2 systems. The catalytic activity studies using HP-CNTs alone, did not produce any product. It was probably due to the fact that adsorption alone cannot facilitate the reaction. It was interesting to note that only the MWCNT/TiO_2 binary nanohybrid systems answered the reaction (Table 5). This is likely to be caused by the inefficiency of the other catalyst systems to respond in the visible region and also probably due to the inefficiency of the metal co-catalysts to induce charge separation to utilize the generated electrons for the photocatalytic reduction. However, minor conversion was obtained with the Pd doped systems. The enhancement of photocatalytic properties of titania and increase of the adsorption of NB in the TCNT(x) hybrids was accounted to the suitable modification of the MWCNT surface. The functionalization is known to serve as good dispersing agents of the metal oxide active phase (TiO_2) [48]. Moreover, the HP-CNTs plays significant role in the effective surface integration and formation of mid band gap states (Ti-O-C linkages) which is already substantiated with the XPS, UVDRS, PL and TEM. Our previous studies on photocatalytic degradation of organic pollutants had revealed that the harsh acid treatment was less efficient than the mild strategy of H_2O_2 functionalization [49]. The hydrogen peroxide functionalized MWCNTs assist the concentration and efficient adsorption of NB through the interactions with the polarized surface induced by the heteroatoms (oxygen

functionalities) [50]. The HP-CNTs possess hydroxyl and carbonyl functional groups on the CNT surface. The HP-CNTs were chosen w.r.t the nitric acid functionalized CNTs (Nf-CNTs), because the carboxylic acid (Nf-CNTs) groups increased the hydrophilicity of the carbon based catalyst but nitrobenzene is a hydrophobic reagent. As a result, the existence of carboxylic groups hindered the adsorption of nitrobenzene [12]. The HP-CNTs exhibited the multifunctional role of absorptive sites (surface defects and conjugated π systems), diffusive sites (active sites or hydroxyl, carbonyl groups attached to the surface function as diffusing the absorbed NB to the photocatalytic titania defect sites). Furthermore, the physisorption of NB at the surface of HP-CNTs did not influence the charge transfer properties of CNTs [51].

The photocatalytic reduction of NB under visible light irradiation was probed employing different catalyst systems and the results are presented in Table 5. Among the various binary hybrids of varying MWCNT content, the TCNT(0.5) catalysts exhibited the maximum efficiency. The excessive content of MWCNTs in the MWCNT/TiO_2 binary composites would have a detrimental effect on the photocatalytic efficiency since it would result in the elevated scattering and absorption of photons[52]. The TCNT(0.5) catalyst was prepared by the incorporation of 0.5 wt. % of hydrogen peroxide functionalized MWCNTs (HP-CNTs) by the one-pot template free hydrothermal method. The optimum content of the HP-CNTs and efficient preparation method brought about effective surface integration (evident from XPS and UVDRS) between the MWCNTs and TiO_2. The HP-CNTs in the binary hybrid system reduced the rate of charge carrier recombination or enhanced the charge separation at TiO_2 sites. This was confirmed by the PL spectra (Fig. 3). The TCNT(x) photocatalysts reduce the adsorbed NB molecules to aniline by accepting the photo-generated electrons with prolonged life span.

The TCNT(0.5) photocatalyst system possess a greater extent of oxygen vacancy (Ov) sites on TiO_2, which was indicated in the PL spectra (Fig.3). These defect sites are known for enhancing the adsorption of NB through the oxygen of the nitro group, to compensate for the

oxygen vacancy [50]. Herein, the XPS spectra reveal the presence of electron trap sites like Ti^{3+} and formation of intermediate states (Ti-O-C linkages) in the TiO_2 bandgap via carbon doping. Also the HP-CNTs with conjugated sp^2 hybrid network are known to its function of formation of heterojunction (XPS, PL and UVDRS) [53].The significant visible light absorption and photocatalytic activity of the TCNT(0.5) system can be attributed to the formation of Ti-O-C bonds/intermediate states in the bandgap of TiO_2 which is confirmed by the UV-Vis DRS and XPS spectra. This formation of mid-band gap states in the titania lattice is known to enhance the visible light absorption considerably [34].Enhanced specific surface area, large pore diameter and better pore volume of the photocatalyst (from BET analysis) also contributed to the better photocatalytic performance of the TCNT(0.5) system.

Table 5 Effect of catalyst systems prepared on reduction of NB to aniline

The effect of various alcohols as solvents was analysed on the reduction of NB and it is presented in Figure S5. It was observed that IPA exhibited better conversion of nitrobenzene to aniline (89 %) than ethanol (53%) & methanol (68%).

The main criteria for the photocatalytic reduction to occur is that the CB minimum of the semiconductor should be more negative w.r.t the reduction potential of the substrate. Here in, the reaction of photocatalytic reduction of nitrobenzene (NB) to aniline is thermodynamically feasible as the reduction potential of NB is [E of $C_6H_5NO_2/C_6H_5NH_2$ = -0.486 V vs. NHE] lower than the CB potential of TiO_2. The NB reduction potential is -0.5 V vs SCE and CB potential of anatase TiO_2 is -0.85 V vs SCE [54]. The studies by Ferry *et al.* have also proposed that the photoreduction of the nitroaromatic compounds in alcohol solvents is brought about by the electrons at the TiO_2 surface (electron traps (Ti^{3+}) or defect sites) rather than the secondary alcohol radicals [55–57].

The photocatalytic evaluation employing the TCNT(0.5) catalyst showed enhancement in the formation of aniline with time (Fig. S6). The NB conversion to aniline was observed to be complete (100 %) after 40 minutes . The single peak in the GC-MS spectra showed the 100 % selectivity of the prepared photocatalyst (Fig. S7). The catalyst amount was optimized to be 0.035 g (Fig. S8).

The efficient TCNT(0.5) photocatalyst was tested for its reusability (Fig. S9) in the reduction of NB. It was found that there was no significant loss of photocatalytic activity and selectivity , even after 4 runs.

Photocatalytic Reaction Pathway of NB reduction to Aniline under Visible Light

In the proposed photocatalytic reduction of nitrobenzene (NB) to aniline under visible light, using a TiO_2–CNT hybrid catalyst (e.g., TCNT(0.5)) and isopropanol (IPA) as a hole scavenger, the overall mechanism can be understood as follows. Initially, NB molecules adsorb onto defect-rich, high-purity carbon nanotubes (CNTs) via π–π interactions and through surface functionalities such as hydroxyl and carbonyl groups (of HP-CNTs) that direct the adsorbed molecules toward the TiO_2 sites. Preferential adsorption onto TiO_2 occurs at defect and oxygen vacancy sites, which are known to enhance reactant binding and activation [50]. Under visible-light irradiation, the Ti–C and Ti–O–C bonds formed in the TiO_2–CNT nanohybrid introduce mid-bandgap states, effectively narrowing the bandgap of TiO_2 and extending its light absorption into the visible region. This defect/doping-driven band structure modification enhances the charge carrier dynamics, as photogenerated electrons are efficiently transferred to the CNTs, which serve as electron reservoirs, thereby limiting electron–hole recombination and improving the overall photoactivity.

Once generated, the photogenerated electrons stored in the CNTs are readily available to reduce the NB molecules. Classical reduction pathways of NB to aniline typically involve the

formation of transient intermediates, such as nitrosobenzene and phenylhydroxylamine, before the final conversion to aniline [58,59]. These intermediates benefit from the prolonged electron lifetime and high electron flux facilitated by the TiO₂–CNT interface, where CNTs' excellent electrical conductivity and defect sites of the CNTs help shuttle and stabilize electrons. Meanwhile, photogenerated holes in TiO₂ are scavenged by IPA, which is oxidized to acetone, releasing protons that participate in the reduction process. Thus, IPA not only prevents electron–hole recombination but also provides a proton source, which is crucial for the stepwise reduction of NB to aniline. Conducting the reaction under a nitrogen atmosphere further enhances the selectivity, as it prevents the formation of superoxide radicals from oxygen, thereby minimizing undesired side reactions and ensuring the efficient conversion of NB to aniline. The defect-engineered TiO₂–CNT nanohybrid efficiently harvests visible light, generates and stabilizes charge carriers, and, in combination with IPA as a hole scavenger and proton donor, drives the stepwise reduction of NB to aniline via known intermediates with minimal electron–hole recombination and side reactions.

Fig. 7 Schematic diagram illustrating the NB reduction under visible light with IPA as the proton donor/hole scavenger employing the MWCNT/TiO₂ binary nanohybrid

3.2.2 Redox synthesis of benzimidazoles

In 1997, Wang *et al.* reported the combined photocatalytic redox synthesis of benzimidazoles via the reduction of *ortho*-dinitrobenzene and the oxidation of alcohols in the presence of TiO₂ photocatalyst under UV light irradiation. The benzimidazole synthesis is a multistep process in which the unique bicentric (oxidation centre and reduction centre) feature of the illuminated semiconductor photocatalyst is exploited. The efficient charge separation in the photocatalyst would generate micro-environment that possess both reduction site (CB electron) and an oxidation site (VB hole). The formed intermediates from one site would turn

out to be the substrate for the other site. The integration of both reaction sites would complete the sophisticated multistep synthesis in one pot [60].

Shiraishi *et al*. in 2010 investigated the one-pot synthesis of benzimidazoles employing Pt@TiO$_2$ photocatalysts under inert conditions with light irradiation of wavelength greater than 300 nm. They demonstrated that the multistep one pot synthesis proceeded through the coupled effect of photocatalysis and catalysis. The TiO$_2$ assisted the photocatalytic oxidation of alcohol to aldehyde, while the Pt nanoparticle at the surface contributed to the dehydrogenation of the benzimidazoline intermediates formed after the condensation of *ortho*-phenylenediamine (OPdA) and alcohol [61].However, the direct one-pot synthesis of benzimidazole from *ortho*-nitroaniline (ONA) is considered more atom economic as it forms the precursor for *ortho*-phenylenediamines (OPdA) and *ortho*-dinitrobenzenes. In 2011, Selvam *et al*. studied the UV and solar light assisted synthesis of benzimidazole using Pt doped TiO$_2$ as the photocatalyst. However, the conversion was comparatively low under solar light irradiation [62]. Another report in 2012, by the same group reported that the condensation between the amino group and aldehyde was the rate limiting step in the reaction. They demonstrated that the yield from IPA as the substrate/solvent, was too low as the corresponding oxidation product acetone formed, slowed down the condensation step due to steric effect. Also, they revealed that the use of methanol produced low yield, as a consequence of hemiacetal formation as the major oxidation product along with formaldehyde. The report also depicted that the doped systems (Pt, N, Ag, Pd, Ru etc.) outperformed the prepared TiO$_2$ in the anatase and rutile phase and other semiconductors like ZnO, CdS and Fe$_2$O$_3$ in the reaction under UV light irradiation. However, the reactivity of all the systems were lower w.r.t the standard Degussa p25 [63].

Herein, a simple, robust one-pot photocatalytic redox synthesis of benzimidazoles from ortho-nitroaniline (ONA) and alcohol as substrates is reported employing the fabricated binary MWCNT/TiO$_2$ nanohybrid systems. To the best of our knowledge, this is the first report on

visible light driven, metal (usually, Pt was used) and acid free photoredox catalysis for synthesis of benzimidazoles at room temperature and atmospheric pressure. This photocatalytic pathway employing hydrogen peroxide functionalized MWCNT (HP-CNTs) doped TiO_2 binary nanohybrid catalysts emerge to be an atom economic (ONA is precursor of OPdA), environmentally benign (alcohol as solvent and substrate), cost effective (noble metal free and simple reagents), energy efficient (RT and 1 atm), highly selective & efficient strategy for the production of these essential pharmacophores.

The incorporation of hydrogen peroxide functionalized MWCNTs in TiO_2 matrix is primarily responsible for the superior efficiency of this photocatalytic redox reaction. As already discussed, (section 3.2.1: NB reduction), they contribute to the visible light sensitivity by shifting the absorption edge to the visible region via, C doping/Ti-O-C bond formation or by serving as sensitizers. The better substrate (nitroarenes) adsorption properties due to the presence of hydroxyl and carbonyl surface functionalities and excellent charge transfer properties of the HP-CNTs further influence the photocatalytic efficiency of the binary hybrid system in the combined photoredox synthesis of benzimidazoles [12, 51]. The effect of reaction conditions, various catalyst systems, solvents, catalyst amount, time etc. were investigated. Here, alcohols perform multifunctional role of substrate, proton donor, hole scavenger and also as solvent for the reaction. Unlike the previous reports in literature, our work demonstrates excellent conversion and selectivity with methanol and IPA as the substrates, which is not reported elsewhere.

Visible light irradiation of ethanolic solution of ONA alone, generated no reaction product suggesting that the presence of photocatalyst was indispensable for the reaction. On the other hand, no product was detected when the redox reaction was carried out in the absence of light. The studies revealed that the reaction was feasible under air, O_2 and N_2 atmospheres (Table 6, entries 3,4 and 5). However, the photocatalytic efficiency was found to be better under N_2

atmosphere. Conversion of 93 % was achieved under N_2 atmosphere (closed reactor) when the light intensity was only 0.02 W/cm^2, while under air/O_2 atmosphere (open reactor) with 0.05 W/cm^2 light intensity, only 79 % conversion was attained. This can be attributed to the better feasibility of reduction of imine intermediate to hydroxyl amine (Fig. S10) under N_2 atmosphere, as there are no superoxide anions to compete at the reduction site. The further investigations were carried out under inert atmosphere.

Table 6 Effect of reaction conditions on the redox synthesis of benzimidazoles

Influence of Alcohols as Substrates/solvents

When the reaction was carried out in ethanol as substrate/solvent, 2-methyl benzimidazole [m/z=132] was the only product obtained (Fig. 8, Fig. S11). This was consistent with other reports in literature, where TiO_2 was used as photocatalyst. The reaction employing MWCNT/TiO_2 binary hybrids under visible light irradiation exhibited complete selectivity and the reaction pathway was similar to that of TiO_2 [63].

The combined photocatalytic redox reaction when performed with ONA and IPA as substrates yielded two products mainly; 2-methyl benzimidazole [m/z=132] and methyl, propionic acid substituted benzimidazoles (mpas-BI) [m/z=204.1] with a selectivity of 58 % and 42 % respectively (Fig. 9). The probable isomeric products of mpas-BI were 3-(1-methyl-1H-benzoimidazol-2-yl)-propionic acid (A), 3-(2-Methyl-1H-benzimidazol-1-yl) propanoic acid (B) and 2-(2-Methylbenzimidazol-1-yl) propanoic acid(C) (Fig. S12). Distinct from the reports available in literature, excellent conversion and selectivity was obtained employing methanol as the substrate/solvent. The methoxymethyl benzimidazole [m/z=162] was the only product obtained (Fig. 10). The probable isomers with the same [m/z=162] value obtained from the GC-MS spectra include 1-(methyloxymethyl)-benzimidazole [(A) m/z=162] 2-(methoxymethyl)-1H-benzoimidazole [(B) m/z=162] (Fig. S13).

The confirmation of obtained products (substituted benzimidazoles) is still a matter of dispute, as its isolation and determination were beyond the scope of our current study. However, the combined redox synthesis carried out employing MWCNT/TiO$_2$ binary nanohybrids generated substituted benzoimidazoles with better yield and high selectivity. Moreover, the incorporation of hydrogen peroxide functionalized MWCNTs (HP-CNTs) and the preparation method (hydrothermal synthesis) highly influenced the formation of specific products. The formation of substituted benzimidazoles was highly influenced by the photocatalytic oxidation product in the first step.

Considering the photocatalytic redox reaction between ONA and methanol, the probable oxidation products of methanol (1st step) include formaldehyde, dimethyl ether, methyl formate, dimethoxymethane etc. The chances for further condensation of these oxidized species cannot be ruled out in this photocatalytic process involving various free radical formations. Several factors including the phase orientation, surface defects and other factors influence the oxidation products. A plausible reaction pathway for this reaction is suggested below (Fig. 11). However, detailed mechanistic studies have to be carried out to determine the exact reaction pathway.

Effect of Initial Concentration of ONA

Studies were performed to optimize the concentration of ONA in the reaction employing the TCNT(0.5) photocatalyst. The concentration of 0.5 mM was determined to be the optimum, under N$_2$ atmosphere and visible light irradiation (Table 7).

Table 7 Effect of ONA concentration on the redox synthesis of benzimidazole

Photocatalytic Efficiency of Various MWCNT/TiO$_2$ Binary Nanohybrids

The investigations of combined photoredox synthesis of benzimidazoles from ONA and ethanol employing various photocatalyst systems prepared are depicted in Table 8. The photocatalytic efficiency of the prepared MWCNT/TiO$_2$ binary hybrid systems were compared

with the standard Aldrich titania, lab synthesized bare TiO_2, transition metal modified $TiO_2$and

transition metal/MWCNT modified TiO_2 ternary nanohybrids. Similar to the results of NB

reduction, the functionalized MWCNT (HP-CNT) incorporated TiO_2 exhibited superior

photocatalytic efficiency in comparison with other catalysts. The standard Sigma Aldrich titania

did not answer the reaction, probably due to the visible light insensitivity. On the other hand, the

hydrothermally prepared lab TiO_2 exhibited low conversion (34 %), and also the transition metal

modified TiO_2 and other $TM/MWCNT/TiO_2$ ternary nanohybrids were not effective

photocatalysts for the reaction. This may be attributed to the poor absorption of substrate species

(ONA and alcohol), inferior reduction potential [evidenced in section 3.2.1 [(NB reduction), Here,

(imine (I) to hydroxyl amine (II), (Fig. S10)], poor charge separation characteristics and lack of

absorption under visible light spectra. However, 34 % conversion was attained employing the Pd

doped MWCNT/TiO_2 ternary hybrids. The reaction pathway employing TiO_2 is depicted in Fig.

S10. The TCNT(0.5) photocatalyst showed maximum efficiency and complete conversion to

benzimidazole in a short period of 35 minutes.

Table 8 Effect of various photocatalyst systems prepared on the redox synthesis of

benzimidazoles

The high rate of conversion and excellent selectivity of the MWCNT modified TiO_2

systems can be attributed to several factors. Primarily, the specific adsorption properties of these

carbon nanostructures lead to the formation of specific products in the reaction. It is supposed

to influence all stages of the reaction, beginning with the oxidation of the alcohol species,

followed by the condensation and formation of imines, reduction of the imine species to

hydroxyl amine, and final dehydration step (Fig. S10). The effective charge separation

characteristics [discussed in section 3.2.1] provide the better distinction of redox sites and assist

the quick formation of products (35 min) with high selectivity. Moreover, the functionalized

MWCNTs in the binary nanohybrid photocatalyst systems form Ti-O-C intermediate states and

shift the response of TiO_2 to the visible region (evident from XPS spectra and UV-Vis DRS (Fig. 6 and Fig. 2 respectively)).

Fig. S14 depicts the effect of time on combined redox synthesis of benzimidazoles from ONA and ethanol as substrates. Complete conversion of ONA was obtained in about 35 minutes with 100 % selectivity.

The MWCNT/TiO_2 binary nanohybrids are determined to be highly efficient photocatalyst in the combined redox synthesis of substituted benzimidazoles. The Sigma Aldrich titania was not photocatalytically active for this reaction under the visible light irradiation. However, the lab synthesized TiO_2 exhibited very low conversion. The specific adsorption characteristics and charge separation efficiency of hydrogen peroxide functionalized MWCNTs make them potential cocatalysts in the photocatalytic combined redox synthesis. The PL spectra, UV-Vis DRS, XPS spectra etc. further underlined our inferences. There is no application of toxic reagents that are generally employed in the synthesis of these potential pharmacophores.

Conclusion

In conclusion, green and robust MWCNT/TiO_2 nanohybrid photocatalysts with hydrogen peroxide functionalized MWCNTs (HP-CNTs) as co-catalysts were prepared employing template free hydrothermal method. The catalyst system exhibited excellent conversion and selectivity in the reduction of nitrobenzene to aniline and in the redox synthesis of benzimidazoles under visible light irradiation. The surface hydroxyl and carbonyl groups on the functionalized HP-CNT surface accounted for the effective adsorption and diffusion of the nitroarenes on the surface. The formed heterojunctions assisted the better separation of charge carriers. The presence of Ti-O-C intermediate state and electron trap sites prolonged the electron life time at the surface that was responsible for the excellent conversion of NB and

ONA into desired products in the alcohol medium, in the studied reactions. The optimum HP-CNT content (0.5 wt. %) had significant effect on the optical and textural characteristics of the nanohybrid which is evidently revealed by UV-visible DRS, BET measurements, TEM, SEM, XPS etc. Furthermore, the significance and influence of optimum content of MWCNTs in the photocatalytic activity studies is unveiled with clarity. Thus, the synergistic effect of HP-CNT coupled with the superior photocatalytic properties of TiO_2 has brought about the enhanced photocatalytic activity in the investigated reactions.

Acknowledgement

References

[1]   S. Chen, H. Zhang, X. Fu, Y. Hu, Preparation, characterization, and photocatalytic performance of Ce_2S_3 for nitrobenzene reduction, Appl. Surf. Sci. 275 (2013) 335–341.

[2]   A.H. Qusti, R.M. Mohamed, M.A. Salam, Photocatalytic synthesis of aniline from nitrobenzene using Ag-reduced graphene oxide nanocomposite Photocatalytic synthesis of aniline from nitrobenzene using Ag-reduced graphene oxide nanocomposite, Ceram. Int. 40 (2014) 5539–5546.

[3] G. Mariappan, R. Hazarika, F. Alam, R. Karki, U. Patangia, S. Nath, Synthesis and biological evaluation of 2-substituted benzimidazole derivatives, Arab. J. Chem., 8 (2015) 715–719.

[4] S.I. Alaqeel, Synthetic approaches to benzimidazoles from *o*-phenylenediamine: A literature review, J. Saudi Chem. Soc., 21 (2017) 229–237.

[5] A.H. Qusti, R.M. Mohamed, M.A. Salam, Photocatalytic synthesis of aniline from nitrobenzene using Ag-reduced graphene oxide nanocomposite, Ceram. Int., 40 (2014) 5539–5546.

[6] S. Park, J. Jung, E.J. Cho, Visible-Light-Promoted Synthesis of Benzimidazoles, European J. Org. Chem., 2014 (2014) 4148–4154.

[7] G. Han, Y. Sun, Visible-light-driven organic transformations on semiconductors, Mater. Today Phys., 16 (2021) 100297.

[8] J. Wen, J. Xie, X. Chen, X. Li, A review on g-C$_3$N$_4$-based photocatalysts, Appl. Surf. Sci., 391(2017) 72-123.

[9] W. Han, Z. Li, Y. Li, X. Fan, F. Zhang, G. Zhang, W. Peng, The Promoting Role of Different Carbon Allotropes Cocatalysts for Semiconductors in Photocatalytic Energy Generation and Pollutants Degradation. Front. Chem. 5(2017)84.

[10] L. H Zhang, Y. Shi, Y. Wang, N. R Shiju, Nanocarbon Catalysts: Recent Understanding Regarding the Active Sites. *Adv. Sci.* 7 (2020) 1902126.

[11] S. Wu, G. Wen, R. Schlogl, D.S. Su, Carbon nanotubes oxidized by a green method as efficient metal-free catalysts for nitroarene reduction, Phys. Chem. Chem. Phys. 17 (2015) 1567–1571.

[12] S. Wu, G. Wen, B. Zhong, B. Zhang, X. Gu, N. Wang, Reduction of nitrobenzene catalyzed by carbon materials, Chinese J. Catal. 35 (2014) 914–921.

[13] H. Fu, D. Zhu, Graphene oxide-facilitated reduction of nitrobenzene in sulfide-containing aqueous solutions, Environ. Sci. Technol. 47 (2013) 4204–4210.

[14] H. Hu, J.H. Xin, H. Hu, X. Wang, Structural and mechanistic understanding of an active

and durable graphene carbocatalyst for reduction of 4-nitrophenol at room temperature, Nano Res. 8 (2015) 3992–4006.

[15] H. Wang, H.L. Wang, W.F. Jiang, Z.Q. Li, Photocatalytic degradation of 2,4-dinitrophenol (DNP) by multi-walled carbon nanotubes (MWCNTs)/TiO_2 composite in aqueous solution under solar irradiation, Water Res. 43 (2009) 204–210.

[16] Y. Panahian, N. Arsalani, Synthesis of Hedgehoglike F-TiO_2(B)/CNT Nanocomposites for Sonophotocatalytic and Photocatalytic Degradation of Malachite Green (MG) under Visible Light: Kinetic Study, J. Phys. Chem. A. 121 (2017) 5614–5624.

[17] K. Dai, X. Zhang, K. Fan, P. Zeng, T. Peng, Multiwalled Carbon Nanotube-TiO_2 Nanocomposite for Visible-Light-Induced Photocatalytic Hydrogen Evolution, J. Nanomater. 2014 (2014) 1–8.

[18] F.H. Abdulrazzak, F.H. Hussein, A.F. Alkaim, I. Ivanova, A. V Emeline, D.W. Bahnemann, Sonochemical/hydration–dehydration synthesis of Pt–TiO_2NPs/decorated carbon nanotubes with enhanced photocatalytic hydrogen production activity, Photochem. Photobiol. Sci. 15 (2016) 1347–1357.

[19] H. Fu, D. Zhu, Graphene oxide-facilitated reduction of nitrobenzene in sulfide-containing aqueous solutions, Environ. Sci. Technol. 47 (2013) 4204–4210.

[20] J O. Olowoyo, M. Kumar, S. L. Jain, J. O. Babalola, A. V. Vorontsov, U. Kumar, Insights into Reinforced Photocatalytic Activity of the CNT–TiO_2 Nanocomposite for CO_2 Reduction and Water Splitting, J. Phys. Chem. C, 123 (2019) 367-378.

[21] S. Muduli, W. Lee, V. Dhas, S. Mujawar, M. Dubey, K. Vijayamohanan, S.H. Han, S. Ogale, Enhanced conversion efficiency in dye-sensitized solar cells based on hydrothermally synthesized TiO_2-MWCNT nanocomposites, ACS Appl. Mater. Interfaces. 1 (2009) 2030–2035.

[22] S. Trocino, A. Donato, M. Latino, N. Donato, S.G. Leonardi, G. Neri, Pt-

TiO$_2$/MWCNTs hybrid composites for monitoring low hydrogen concentrations in air, Sensors. 12 (2012) 12361–12373.

[23]   N. Shaari, S.H. Tan, A.R. Mohamed, Synthesis and characterization of CNT/Ce-TiO$_2$ nanocomposite for phenol degradation, J. Rare Earths. 30 (2012) 651–658.

[24] B.K. Vijayan, N.M. Dimitrijevic, D. Finkelstein-shapiro, J. Wu, K.A. Gray, Coupling Titania Nanotubes and Carbon Nanotubes To Create Photocatalytic Nanocomposites, ACS Catal., 2 (2012) 223–229.

[25]   W. Chen, Z. Fan, B. Zhang, G. Ma, K. Takanabe, X. Zhang, Z. Lai, Enhanced visible-light activity of titania via confinement inside carbon nanotubes, J. Am. Chem. Soc. 133 (2011) 14896–14899.

[26] H. Yaghoubi, Z. Li, Y. Chen, H.T. Ngo, V.R. Bhethanabotla, B. Joseph, S. Ma, R. Schlaf, A. Takshi, A. Morais, S. do A. Carminati, A.F. Nogueira, R.K. Manoharan, S. Sankaran, Nanostructured hybrid materials based on reduced graphene oxide for solar energy conversion, ACS Catal. 9923 (2016) 992314.

[27] Y. Panahian, N. Arsalani, Synthesis of Hedgehoglike F-TiO$_2$(B)/CNT Nanocomposites for Sonophotocatalytic and Photocatalytic Degradation of Malachite Green (MG) under Visible Light: Kinetic Study, J. Phys. Chem. A. 121 (2017) 5614–5624.

[28] G. Mamba, X.Y. Mbianda, A.K. Mishra, Photocatalytic degradation of the diazo dye naphthol blue black in water using MWCNT/Gd,N,S-TiO$_2$ nanocomposites under simulated solar light, J. Environ. Sci. (China). 33 (2015) 219–228.

[29]   Y. Panahian, N. Arsalani, Synthesis of Hedgehoglike F-TiO$_2$(B)/CNT Nanocomposites for Sonophotocatalytic and Photocatalytic Degradation of Malachite Green (MG) under Visible Light : Kinetic Study J. Phys. Chem. A., 121 (2017) 5614–5624.

[30] E.T. Mombeshora, R. Simoyi, V.O. Nyamori, P.G. Ndungu, Multiwalled Carbon

Nanotube-titania Nanocomposites : Understanding Nano-Structural Parameters and Functionality in Dye-sensitized Solar Cells, S. Afr. J. Chem., 68 (2015) 153–164.

[31] B. Chai, T. Peng, X. Zhang, J. Mao, K. Li, X. Zhang, Synthesis of C_{60}-decorated SWCNTs (C_{60}-d-CNTs) and its TiO_2-based nanocomposite with enhanced photocatalytic activity for hydrogen production, Dalt. Trans. 42 (2013) 3402–3409.

[32] C. Karunakaran, P. Magesan, P. Gomathisankar, P. Vinayagamoorthy, Absorption, emission, charge transfer resistance and photocatalytic activity of Al_2O_3/TiO_2 core/shell nanoparticles, Superlattices Microstruct. 83 (2015) 659–667.

[33] F.H. Abdulrazzak, F.H. Hussein, A.F. Alkaim, I. Ivanova, A. V Emeline, D.W. Bahnemann, Sonochemical/hydration–dehydration synthesis of $Pt–TiO_2NPs$/decorated carbon nanotubes with enhanced photocatalytic hydrogen production activity, Photochem. Photobiol. Sci. 15 (2016) 1347–1357.

[34] J.C. Gonzalez-torres, E. Poulain, V. Dominguez-soria, R. Garcia-cruz, O. Olvera-neria, C, N, S, and F-Doped Anatase TiO_2 (101) with Oxygen Vacancies: Photocatalysts Active in the Visible Region, Int. J. Photoenergy, 2018 (2018) 7506151.

[35] Y. Zhang, Z. Xing, J. Zou, Z. Li, X. Wu, L. Shen, Q. Zhu, S. Yang, W. Zhou, 3D urchin-like black $TiO_{2−x}$/carbon nanotube heterostructures as efficient visible-light-driven photocatalysts, RSC Adv. 7 (2017) 453–460.

[36] O. Akhavan, R. Azimirad, S. Safa, M.M. Larijani, Visible light photo-induced antibacterial activity of CNT–doped TiO_2 thin films with various CNT contents, J. Mater. Chem. 20 (2010) 7386.

[37] B.K. Vijayan, N.M. Dimitrijevic, D. Finkelstein-Shapiro, J. Wu, K.A. Gray, Coupling titania nanotubes and carbon nanotubes to create photocatalytic nanocomposites, ACS Catal. 2 (2012) 223–229.

[38] L. Xu, L. Yang, E.M.J. Johansson, Y. Wang, P. Jin, Photocatalytic activity and mechanism of bisphenol a removal over TiO_{2-x}/rGO nanocomposite driven by visible light, Chem. Eng. J., 350 (2018) 1043–1055.

[39] W. Ren, Z. Ai, F. Jia, L. Zhang, Low temperature preparation and visible light photocatalytic activity of mesoporous carbon-doped crystalline TiO_2, Appl. Catal. B Environ., 69 (2007) 138–144.

[40] J. Yu, G. Dai, Q. Xiang, M. Jaroniec, Fabrication and enhanced visible-light photocatalytic activity of carbon self-doped TiO_2 sheets with exposed {001} facets, Appl. Catal. B Environ., 21 (2011) 1049–1057.

[41] J. Su, X. Zou, J.-S. Chen, Self-modification of titanium dioxide materials by Ti^{3+} and/or oxygen vacancies: new insights into defect chemistry of metal oxides, RSC Adv. 4 (2014) 13979–13988.

[42] S.P. Pujari, L. Scheres, A.T.M. Marcelis, H. Zuilhof, Covalent Surface Modification of Oxide Surfaces, Angew. Chemie Int. Ed. 53 (2014) 6322–6356.

[43] J. Su, X.-X. Zou, Y.-C. Zou, G.-D. Li, P.-P. Wang, J.-S. Chen, Porous Titania with Heavily Self-Doped Ti^{3+} for Specific Sensing of CO at Room Temperature, Inorg. Chem. 52 (2013) 5924–5930.

[44] K. Li, Z. Huang, X. Zeng, B. Huang, S. Gao, J. Lu, Synergetic Effect of Ti^{3+} and Oxygen Doping on Enhancing Photoelectrochemical and Photocatalytic Properties of TiO_2/g-C_3N_4 Heterojunctions, ACS Appl. Mater. Interfaces. 9 (2017) 11577–11586.

[45] H. Park, S. Liu, P.A. Salvador, G.S. Rohrer, High visible-light photochemical activity of titania decorated on single-wall carbon nanotube, R. Sc Adv., 6 (2016) 22285–22294.

[46] K. Imamura, T. Yoshikawa, K. Hashimoto, H. Kominami, Stoichiometric production of aminobenzenes and ketones by photocatalytic reduction of nitrobenzenes in secondary

alcoholic suspension of titanium (IV) oxide under metal-free conditions Acetone, Applied Catal. B, Environ. 134–135 (2013) 193–197.

[47]   K. Imamura, S. Iwasaki, T. Maeda, K. Hashimoto, B. Ohtani, H. Kominami, Photocatalytic reduction of nitrobenzenes to aminobenzenes in aqueous suspensions of titanium(iv) oxide in the presence of hole scavengers under deaerated and aerated conditions, Phys. Chem. Chem. Phys. 13 (2011) 5114.

[48]   B. Gao, G.Z. Chen, G. Li Puma, Carbon nanotubes/titanium dioxide (CNTs/TiO$_2$) nanocomposites prepared by conventional and novel surfactant wrapping sol–gel methods exhibiting enhanced photocatalytic activity, Appl. Catal. B Environ. 89 (2009) 503–509.

[49]   H. Joseph, S. Sugunan, L. Gurrala, M. Mohan, G. Soumya, New insights into surface functionalization and preparation methods of MWCNT based semiconductor photocatalysts, Ceram. Int. 45 (2019). doi:10.1016/j.ceramint.2019.04.058.

[50] J. Song, Z.F. Huang, L. Pan, K. Li, X. Zhang, L. Wang, J.J. Zou, Review on selective hydrogenation of nitroarene by catalytic, photocatalytic and electrocatalytic reactions, Appl. Catal. B Environ., 227 (2018) 386–408.

[51]   M.D. Ganji, M. Mohseni, Simple benzene derivatives adsorption on defective single-walled carbon nanotubes : a first-principles van der Waals density functional study, J. Mol. Model.,19 (2013) 1059–1067.

[52]   S.Y. Sawant, M.H. Cho, Facile electrochemical assisted synthesis of ZnO/graphene nanosheets with enhanced photocatalytic activity, RSC Adv. 5 (2015) 97788–97797.

[53]   B.H. Nguyen, V.H. Nguyen, D.L. Vu, Photocatalytic composites based on titania nanoparticles and carbon nanomaterials, Adv. Nat. Sci. Nanosci. Nanotechnol. 6 (2015) 033001.

[54]   S.O. Flores, O. Rios-Bernij, M.A. Valenzuela, I. Cordova, R. Gomez, R. Gutierrez,

Photocatalytic reduction of nitrobenzene over titanium dioxide: By-product

identification and possible pathways, Top. Catal. 44 (2007) 507–511.

[55] J.L. Ferry, W.H. Glaze, Photocatalytic reduction of nitro organics over illuminated

titanium dioxide: Role of the TiO_2 surface, Langmuir. 14 (1998) 3551–3555.

[56] A. Hakki, R. Dillert, D.W. Bahnemann, Factors affecting the selectivity of the

photocatalytic conversion of nitroaromatic compounds over TiO_2 to valuable nitrogen-

containing organic compounds, Phys. Chem. Chem. Phys. 15 (2013) 2992.

[57] T. Zhang, L. You, Y. Zhang, Photocatalytic reduction of p-chloronitrobenzene on

illuminated nano-titanium dioxide particles, Dye. Pigment. 68 (2006) 95–100.

[58] Morrissey, C., & He, H. (2018). Silicene catalyzed reduction of nitrobenzene to aniline:

A mechanistic study, Chem. Phys. Lett., 695, 228–234.

[59] Mahata, A., Rai, R. K., Choudhuri, I., Singh, S. K., & Pathak, B. (2014). Direct vs. indirect

pathway for nitrobenzene reduction reaction on a Ni catalyst surface: A density functional

study, Phys. Chem. Chem. Phys., 16(47), 26365–26374.

[60] H. Wang, R.E. Partch, Y. Li, Synthesis of 2-Alkylbenzimidazoles via TiO_2-Mediated

Photocatalysis, J. Org. Chem., 62 (1997) 5222–5225.

[61] Y. Shiraishi, Y. Sugano, S. Tanaka, T. Hirai, One-Pot Synthesis of Benzimidazoles by

Simultaneous Photocatalytic and Catalytic Reactions on Pt@TiO_2 Nanoparticles,

Angew. Chemie - Int. Ed., 49 (2010) 1656–1660.

[62] K. Selvam, M. Swaminathan, An easy one-step photocatalytic synthesis of 1-aryl-2-

alkylbenzimidazoles by platinum loaded TiO_2 nanoparticles under UV and solar light,

sTetrahedron Lett., 52 (2011) 3386–3392.

[63] D. Annadhasan, K. Selvam, M. Swaminathan, A Combined-Redox Synthesis of 2-

Alkylbenzimidazoles from 2-Nitroanilines by Semiconductor Photocatalysis, Synth.

CRediT authorship contribution statement

Honey Mary Joseph: Writing – original draft, Methodology, Investigatio, Formal Analysis **.**

Hariprasad Narayanan: Editing**,** Software, Analysis. **S, Sugunan:** Writing – review & editing, Supervision, Conceptualization.

Declaration of interests

☒ The authors declare that they have no known competing financial interests or personal relationships that could have appeared to influence the work reported in this paper.

Table 1 Prepared binary MWCNT/TiO$_2$ photocatalysts (TCNT(x))

Catalysts prepared	Notation
Hydrothermally prepared TiO$_2$	LTiO$_2$
0.1wt. % Hf-CNT incorporated TiO$_2$	TCNT(0.1)
0.3wt. % Hf-CNT incorporated TiO$_2$	TCNT(0.3)
0.5 wt. % Hf-CNT incorporated TiO$_2$	TCNT(0.5)
0.7wt. % Hf-CNT incorporated TiO$_2$	TCNT(0.7)
1 wt. % Hf-CNT incorporated TiO$_2$	TCNT(1)
5 wt. % Hf-CNT incorporated TiO$_2$	TCNT(5)
10 wt. % Hf-CNT incorporated TiO$_2$	TCNT(10)

Table 2 Absorption edge and band gap energies of TCNT(x) binary hybrids

Catalyst	Absorption edge (λ) nm	Apparent Band gap (eV) (Urbach's tail)
LTiO$_2$	380	3.2
TCNT(0.3)	392	3.1
TCNT(0.5)	400	3.0
TCNT(0.7)	**485**	**-**
TCNT(1)	**590**	**-**
TCNT(5)	**650**	**-**
TCNT(10)	**682**	**-**

Note: *The TCNT(x=0.7-10 wt. %) binary hybrid systems are biphasic and the band gap calculation in this method is not accurate.*

Table 3. Textural characteristics of the prepared TCNT(x) binary nanohybrids

Catalyst	S_{BET} (m²/g)	Pore diameter (Å)	Pore volume (cm³/g)
TCNT(0.3)	193	22.7	0.1208
TCNT(0.5)	195	27.2	0.2720
TCNT(0.7)	175	22.6	0.1088
TCNT(5)	188	22.5	0.1164
TCNT(10)	193	22.3	0.1185
LTiO₂	97	16.2	0.0298

Table 4 Effect of reaction conditions on the reduction of NB to aniline

Catalyst	Time (h)	% conversion
Without catalyst	1	-
Without light	1	-
N₂ atmosphere	1	94
O₂ atmosphere	1	-
Air atmosphere	1	-

Table 5 Effect of catalyst systems prepared in reduction of NB to aniline

Catalyst	Time	% conversion	% selectivity
SATiO₂	2h	-	-
LTiO₂	2h	-	-
MWCNT	2h	-	-
TCNT(0.1)	40 min	68	100
TCNT(0.3)	40 min	94	100
TCNT(0.5)	40 min	100	100

Catalyst	Time	% conversion	
TCNT(0.7)	40 min	96	100
TCNT(1)	40 min	93	100
TCNT(5)	40 min	63	100
TCNT(10)	40 min	54	100
TM/TiO$_2$	4h	-	-
Nf-CNT(0.5)/TiO$_2$	40 min	52	100
TM/TCNT	4h	-	-

Reaction conditions: Catalyst amount (0.035 g), concentration of NB (1 mM), volume (10 ml), solvent (IPA), light source (150 W Xenon ozone free arc lamp), Light flux: 0.02 W/cm^2 (N$_2$) [TM/TiO$_2$(transition metal doped TiO$_2$), TM/TCNT: transition metal doped MWCNT/TiO$_2$ ternary nanohybrid, TM=Ni, Pd, Pt), Nf-CNT: nitric acid functionalized MWCNT]

Table 6 Effect of reaction conditions on the redox synthesis of benzimidazole

Catalyst	Time (min)	% conversion
Without catalyst	45	-
Without light	45	-
N$_2$ atmosphere	45	93
O$_2$ atmosphere	45	79
Air atmosphere	45	74

Reaction conditions: Catalyst amount (0.04 g), concentration of ONA (0.5 mM), volume (10 ml), solvent (ethanol), light source (150 W Xenon ozone free arc lamp), Light flux: 0.02 W/cm^2 (N$_2$), 0.05 W/cm^2 (air, O$_2$), Catalyst used: TCNT(1)

Table 7 Effect of ONA concentration on the redox synthesis of benzimidazoles

Concentration (M)	Time (h)	% conversion
1	1	0
1	3	0
10^{-2}	3	11
10^{-3}	3	36
0.5×10^{-3}	1	100

Reaction conditions: Catalyst amount (0.04 g), Catalyst: TCNT(0.5), volume (10 ml), solvent (ethanol), light source (150 W Xenon ozone free arc lamp), Light flux: 0.02 W/cm^2 (N$_2$)

Table 8. Effect of various photocatalyst systems prepared on redox synthesis of benzimidazoles

Catalyst	Time	% conversion	% selectivity
SATiO$_2$	4h	-	-
LTiO$_2$	35 min	-	-
TCNT(0.1)	35 min	67	100
TCNT(0.3)	35 min	94	100
TCNT(0.5)	35 min	100	100
TCNT(0.7)	35 min	90	100
TCNT(1)	35 min	82	100
TCNT(5)	35 min	68	100
TCNT(10)	35 min	51	100
TM/TiO$_2$	4h	-	-
TM/TCNT	4h	-	-
Pd(1)TCNT(0.5)	35min	34	100

Pd(1)TCNT(0.5)	35min	28	100

Reaction conditions: Catalyst amount (0.04 g), concentration of ONA(0.5 mM), volume (10 ml), solvent (ethanol), light source (150 W Xenon ozone free arc lamp), Light flux: 0.02 W/cm^2 (N$_2$)(TM: Ni, Pt, Ru, Cu)

Graphical abstract

Highlights

➢ Environmentally benign and energy efficient strategy was employed for the photocatalytic reduction of nitrobenzene to aniline and redox synthesis of benzimidazoles, employing green solvents like alcohols, under visible light irradiation.

➢ The adsorption of the substrates by the cocatalyst, HP-CNTs played a very significant role in the feasibility of the reaction.

➢ The synergistic effect of coupling HP-CNTs with the superior photocatalytic properties of TiO$_2$ accounts for the enhanced substrate adsorption, charge separation and visible light activity of the prepared HP-CNT/TiO$_2$ binary nanohybrid systems.

➢ The formation of mid band gap states (Ti-O-C linkages) and superior textural characteristics (surface area, pore volume etc.) contributed to the better performance of the catalyst.

➢ The structure-activity correlation was well established employing the characterization methods (PL, XPS, UV-Vis DRS, TEM etc.).